

Persistent spin current in mesoscopic ferrimagnetic spin ring

Jing-Nuo Wu,¹ Ming-Che Chang,¹ and Min-Fong Yang²

¹*Department of Physics, National Taiwan Normal University, Taipei, Taiwan*

²*Department of Physics, Tunghai University, Taichung, Taiwan*

(Dated: May 1, 2019)

Using a semiclassical approach, we study the persistent magnetization current of a mesoscopic ferrimagnetic ring in a nonuniform magnetic field. At zero temperature, there exists persistent spin current because of the quantum fluctuation of magnons, similar to the case of an antiferromagnetic spin ring. At low temperature, the current shows activation behavior because of the field-induced gap. At higher temperature, the magnitude of the spin current is proportional to temperature T , similar to the reported result of a ferromagnetic spin ring.

PACS numbers: 75.10Jm, 75.10Pq, 75.30Ds, 73.23Ra

I. INTRODUCTION

Persistent charge current in a mesoscopic metal ring was predicted¹ and observed² a decade ago. In such a ring threaded by a magnetic flux, if the phase coherence length of electrons is larger than the size of the ring, then the electrons can pick up an Aharonov-Bohm (AB) phase after circling the ring once. Such a phase lag (or advance) would lead to a persistent current, which is a periodic function of the threaded magnetic flux,³ and can be detected via the magnetic response of the (isolated) ring. The phase lag (or advance) can also be of geometric origin (Berry phase).⁴ It has been proposed that a Berry phase can appear for an electron moving around the metal ring that subject to a textured magnetic field (or magnetization).⁵ This geometric phase, which depends upon the solid angle associated with the textured magnetic field, can lead to persistent charge and spin currents.⁵ A similar geometric phase appears due to the spin-orbit interaction in one-dimensional rings,^{6,7} which is a manifestation of the Aharonov-Casher (AC) effect.⁸ More studies on the persistent current related to the AC effect can be found in Refs. 9,10,11.

With the advance of spintronics and quantum computation,¹² it becomes more important to understand the behavior of the spin current. Among these investigations, spin transport in pure spin systems plays a special role since there is no complication from charge degrees of freedom. In a recent paper, using a semiclassical spin wave analysis, Schütz *et al.* predicted the existence of persistent spin current in a mesoscopic ferromagnetic (FM) spin ring in a *nonuniform* magnetic field.¹³ The FM spin ring being considered is a charge insulator with Heisenberg spin interaction, and the spin current is carried by magnon excitations. Similar to the case of charge transport in a metal ring subject to a textured magnetic field,⁵ the magnon in a mesoscopic FM spin ring acquires a geometric phase from the (nonuniform) spin texture of the classical ground state. The persistent current is found to be zero at temperature $T = 0$, and proportional to T when $k_B T$ is larger than the field-induced energy gap of the magnons.

Similar method has been applied to an antiferromagnetic (AFM) spin ring with a Haldane gap.¹⁴ As compared with the FM case, there are some subtleties in using the semiclassical method in the AFM case. Due to the problem of infrared-diverging magnetization, the spin-wave approach is not valid for AFM spin chains with half-integer spins.¹⁴ That is the reason why only the integer-spin cases are considered in Ref. 14. Nonetheless, in the integer-spin case, an additional staggered field in the direction of the classical magnetization vectors still has to be introduced. Its value needs to be determined self-consistently before quantitative predictions can be made. The authors of Ref. 14 find that, unlike the case of the FM spin ring, the persistent spin current in an AFM spin ring can be nonzero at $T = 0$ due to quantum fluctuations. When the spin correlation length is much longer than the size of the ring, the magnitude of the spin current exhibits sawtooth variation with respect to the geometric phase, similar to the case of persistent charge current in a metal ring. Recently, the investigation has been extended to an anisotropic FM spin ring,¹⁵ a spin-1/2 AFM spin ring,^{16,17} and an anisotropic AFM spin ring.¹⁸

In this paper, we study the persistent spin current in a ferrimagnetic (FIM) spin ring with alternating spins S^A and S^B under a textured magnetic field. Contrary to the AFM case, the problem of infrared-diverging magnetization does not exist in the present FIM case, no matter whether the constituent spins are integer or half-integer.^{19,20,21,22} Thus the self-consistently determined staggered field needs not be introduced, and physical quantities can be calculated directly as long as system parameters are known. We find that the FIM spin ring can have either FM or AFM characteristics. For example, a quantity proportional to $|S^A - S^B|$ plays a role similar to the Haldane gap in the AFM spin ring. Moreover, a nonzero spin current exists at $T = 0$, again similar to the case of the AFM spin ring.¹⁴ On the other hand, when the thermal energy is higher than the field-induced gap, the magnitude of the spin current is proportional to temperature T , similar to the case in the FM spin ring.¹³

This paper is organized as follows: We present the spin-wave analysis in Sec. II. The results of numerical calcula-

tions are shown in Sec. III, and Sec. IV is the conclusion.

II. THEORETICAL ANALYSIS

The Hamiltonian of the ferrimagnetic Heisenberg spin ring in a nonuniform magnetic field $\vec{h}_j \equiv g\mu_B\vec{B}(\vec{r}_j)$ is

$$H = J \sum_{j \in A \cup B} \vec{S}_j \cdot \vec{S}_{j+1} - \sum_{j_1 \in A, j_2 \in B} \left(\vec{h}_{j_1} \cdot \vec{S}_{j_1}^A + \vec{h}_{j_2} \cdot \vec{S}_{j_2}^B \right), \quad (1)$$

where $J > 0$, and the index j refers to one of the alternating j_1, j_2 sites. That is, sublattice-A can be labelled either by j (an odd integer) or $j_1 = (j+1)/2$; sublattice-B can be labelled by j (an even integer) or $j_2 = j/2$. There are even number of lattice sites N . The length of the ring is L and the lattice spacing $a = L/N$. Periodic boundary condition $\vec{S}_{j+N} = \vec{S}_j$ is used. On the classical level, \vec{S}_j are replaced by classical vectors $S\hat{m}_j$. The classical ground state $\{\hat{m}_j\}$ can be determined from angular variations with respect to each \hat{m}_j , which give

$$\begin{aligned} JS^B(\hat{m}_{j_2-1} + \hat{m}_{j_2}) - \vec{h}_{j_1} + \lambda_{j_1}^A \hat{m}_{j_1} &= 0, \\ JS^A(\hat{m}_{j_1} + \hat{m}_{j_1+1}) - \vec{h}_{j_2} + \lambda_{j_2}^B \hat{m}_{j_2} &= 0, \end{aligned} \quad (2)$$

where λ_j are Lagrange multipliers. It shows that the magnetization aligns parallel to the sum of external and exchange field, as expected. If the Zeeman energy is much smaller than the exchange energy between spins, then \hat{m}_j^A and \hat{m}_{j+1}^B would be nearly antiparallel to each other, as shown in Fig. 1(a). Moreover, due to nonzero magnetization in the present FIM model, \hat{m}_j^A would lie nearly along the direction of \vec{h}_j , instead of nearly perpendicular to \vec{h}_j as in the AFM case¹⁴ (we take $S^A > S^B$ in this paper).

When quantum fluctuations are considered, following the treatment introduced by Schütz *et al.*,^{13,14} each spin operator is expanded using unit vectors that form an orthogonal triad $\{\hat{e}_j^1, \hat{e}_j^2, \hat{m}_j\}$,

$$\vec{S}_j = S_j^\parallel \hat{m}_j + \frac{1}{2} (S_j^+ \hat{e}_j^- + S_j^- \hat{e}_j^+), \quad (3)$$

where $\hat{e}_j^\pm \equiv \hat{e}_j^1 \pm i\hat{e}_j^2$. We focus on systems with large spins (which could be integer or half-integer), and introduce the Holstein-Primakoff bosons a_j, b_j ,

$$\begin{aligned} S_j^{A\parallel} &= S^A - a_j^\dagger a_j, & S_j^{A+} &\cong \sqrt{2S^A} a_j^\dagger; \\ S_j^{B\parallel} &= S^B - b_j^\dagger b_j, & S_j^{B+} &\cong \sqrt{2S^B} b_j^\dagger. \end{aligned} \quad (4)$$

Substituting these into Eq. (1), we obtain $H = H^\parallel + H^\perp + H'$ with

$$H^\parallel = J \sum_{j \in A \cup B} S_j^\parallel S_{j+1}^\parallel - \sum_{j \in A \cup B} S_j^\parallel \hat{m}_j \cdot \vec{h}_j, \quad (5)$$

$$H^\perp = J \sum_{j \in A \cup B} \vec{S}_j^\perp \cdot \vec{S}_{j+1}^\perp, \quad (6)$$

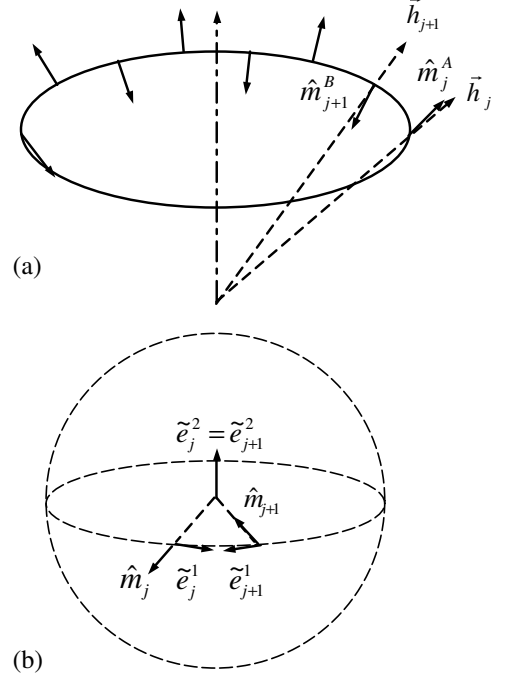


FIG. 1: (a) Classical spin configuration of a FIM spin ring in a crown-shaped magnetic field. (b) Relative orientation for adjacent local triads. The condition $\hat{e}_j^2 = \hat{e}_{j+1}^2 = \hat{m}_j \times \hat{m}_{j+1} / |\hat{m}_j \times \hat{m}_{j+1}|$ is imposed. The circle in the middle is the equator of the sphere.

$$\begin{aligned} H' &= \sum_{j_1 \in A, j_2 \in B} \left\{ \vec{S}_{j_1}^{A\perp} \cdot \left[JS^B(\hat{m}_{j_2-1} + \hat{m}_{j_2}) - \vec{h}_{j_1} \right] \right. \\ &\quad \left. + \vec{S}_{j_2}^{B\perp} \cdot \left[JS^A(\hat{m}_{j_1} + \hat{m}_{j_1+1}) - \vec{h}_{j_2} \right] \right\} \\ &\quad + O(\sqrt{S}). \end{aligned} \quad (7)$$

H^\parallel and H^\perp are of the orders of $O(S^2)$ and $O(S)$ respectively. To the order of $O(S)$, H' is zero because of Eq. (2) and will be neglected in the following. In order to simplify the Hamiltonian, we choose the local triads with the *connection* shown in Fig. 1(b), in which $\hat{e}_j^2 = \hat{e}_{j+1}^2 = \hat{m}_j \times \hat{m}_{j+1} / |\hat{m}_j \times \hat{m}_{j+1}|$ (this is referred to as a choice of gauge). Such *parallel transported* triads are related to the original local triads by local rotations (gauge transformations), $\hat{e}_j^\pm = e^{\pm i\omega_{j \rightarrow j+1}} \hat{e}_{j+1}^\pm$, where $\omega_{j \rightarrow j+1}$ is the angle of rotation around \hat{m}_j that takes \hat{e}_{j+1}^2 to \hat{e}_j^2 .²³

Using the new triads in the Hamiltonian, we obtain

$$H^\parallel = H_c - J \sum_j \hat{m}_j \cdot \hat{m}_{j+1} \left[S^A (b_j^\dagger b_j + b_{j+1}^\dagger b_{j+1}) \right]$$

$$\begin{aligned}
& + S^B \left(a_j^\dagger a_j + a_{j+1}^\dagger a_{j+1} \right) \\
& + \sum_{j_1, j_2} \left(h_{j_1}^A a_{j_1}^\dagger a_{j_1} + h_{j_2}^B b_{j_2}^\dagger b_{j_2} \right), \quad (8)
\end{aligned}$$

where $H_c = JS^A S^B \sum_j \hat{m}_j \cdot \hat{m}_{j+1} - \sum_{j_1, j_2} (S^A h_{j_1}^A + S^B h_{j_2}^B)$ with $h_{j_1}^A \equiv \vec{h}_{j_1} \cdot \hat{m}_{j_1}$ and $h_{j_2}^B \equiv \vec{h}_{j_2} \cdot \hat{m}_{j_2}$. Also,

$$\begin{aligned}
H^\perp &= \frac{J}{2} \sqrt{S^A S^B} \\
&\times \sum_{j_1, j_2} \left\{ \left[(1 + \hat{m}_{j_1} \cdot \hat{m}_{j_2}) a_{j_1}^\dagger b_{j_2}^\dagger e^{i(\omega_{j_1 \rightarrow j_2} - \omega_{j_2 \rightarrow j_1})} \right. \right. \\
&\left. \left. + (1 + \hat{m}_{j_2} \cdot \hat{m}_{j_1+1}) a_{j_1+1}^\dagger b_{j_2}^\dagger e^{i(\omega_{j_1+1 \rightarrow j_2} - \omega_{j_2 \rightarrow j_1+1})} \right. \right. \\
&\left. \left. - (1 - \hat{m}_{j_1} \cdot \hat{m}_{j_2}) a_{j_1}^\dagger b_{j_2}^\dagger e^{-i(\omega_{j_1 \rightarrow j_2} + \omega_{j_2 \rightarrow j_1})} \right. \right. \\
&\left. \left. - (1 - \hat{m}_{j_2} \cdot \hat{m}_{j_1+1}) a_{j_1+1}^\dagger b_{j_2}^\dagger e^{-i(\omega_{j_1+1 \rightarrow j_2} + \omega_{j_2 \rightarrow j_1+1})} \right] \right. \\
&\left. + h.c. \right\}. \quad (9)
\end{aligned}$$

As long as the ring is not too small, neighboring spin vectors would be nearly antiparallel to each other [as shown in Fig. 1(a)] with $\hat{m}_j \cdot \hat{m}_{j+1} = -1 + O(1/N)$. This further simplifies the Hamiltonian to be

$$\begin{aligned}
H &= H_c + \sum_{j_1, j_2} \left[(2JS^B + h_{j_1}^A) a_{j_1}^\dagger a_{j_1} + (2JS^A + h_{j_2}^B) b_{j_2}^\dagger b_{j_2} \right] \\
&- J\sqrt{S^A S^B} \sum_{j_1, j_2} \left[a_{j_1}^\dagger b_{j_2}^\dagger e^{-i(\omega_{j_1 \rightarrow j_2} + \omega_{j_2 \rightarrow j_1})} + a_{j_1+1}^\dagger b_{j_2}^\dagger e^{-i(\omega_{j_1+1 \rightarrow j_2} + \omega_{j_2 \rightarrow j_1+1})} + h.c. \right]. \quad (10)
\end{aligned}$$

The hopping of boson- a from site- j_1 to site- $(j_1 + 1)$ acquires a phase $(\omega_{j_1 \rightarrow j_2} + \omega_{j_2 \rightarrow j_1}) - (\omega_{j_2 \rightarrow j_1+1} + \omega_{j_1+1 \rightarrow j_2})$. After circling around the ring once, the boson gains a cumulative phase $\Omega = \sum_{j=1}^N (-1)^{j+1} (\omega_{j \rightarrow j+1} + \omega_{j+1 \rightarrow j})$, which is the holonomy angle of the parallel transport and equals the solid angle extended by the classical spin texture $\{\hat{m}_j\}$.²⁴ It can be shown that

$$\Omega = \text{Im} \log \prod_{j_1=j_2=1}^{N/2} \left(\hat{e}_{j_1}^+ \cdot \hat{e}_{j_2}^+ \hat{e}_{j_2}^- \cdot \hat{e}_{j_1+1}^- \right), \quad (11)$$

which is a gauge-invariant expression because the $\hat{e}_j^+ \hat{e}_j^-$ vectors always appear in pairs (note that $\hat{e}_{N/2+1}^- = \hat{e}_1^-$). Therefore, this cumulative geometric phase Ω is independent of the choices of the local triads.

The phase factors in Eq. (10) can be made implicit by merging with the boson operators. Such new boson operators would satisfy the twisted boundary conditions: $a_{j_1+N/2} = e^{i\Omega} a_{j_1}$, $b_{j_2+N/2} = e^{-i\Omega} b_{j_2}$. With the help of the transformations,

$$a_k = \sqrt{\frac{2}{N}} \sum_{j \in A} e^{-ika_j} a_j, \quad b_k = \sqrt{\frac{2}{N}} \sum_{j \in B} e^{ika_j} b_j, \quad (12)$$

in which

$$k_n = \frac{2\pi}{L} \left(n + \frac{\Omega}{2\pi} \right), \quad n = 0, 1, 2, \dots, \frac{N}{2} - 1,$$

to conform with the twisted boundary condition, the Hamiltonian becomes

$$H = H_c$$

$$\begin{aligned}
& + \sum_k \left(2JS^B + h_q^A \right) a_{k+q}^\dagger a_k + \left(2JS^A + h_q^B \right) b_{k+q}^\dagger b_k \\
& - 2J\sqrt{S^A S^B} \sum_k \left(a_k b_k + a_k^\dagger b_k^\dagger \right) \cos(ka), \quad (13)
\end{aligned}$$

where we have assumed that the applied magnetic field (as well as $\{\hat{m}_j\}$) has only one Fourier component with momentum q to simplify the expression. A crown-shaped magnetic field with azimuthal symmetry has the $q = 0$ component only. For convenience, we consider the crown-shaped magnetic field below. For a large FIM spin ring in a *weak* magnetic field, we also have $h_0^B \cong -h_0^A \equiv -h_0$ [see Fig. 1(a)] with h_0 being positive. With the help of the Bogoliubov transformation,

$$\begin{aligned}
a_k &= \alpha_k \cosh \theta_k + \beta_k^\dagger \sinh \theta_k; \\
b_k^\dagger &= \alpha_k \sinh \theta_k + \beta_k^\dagger \cosh \theta_k, \quad (14)
\end{aligned}$$

and choosing

$$\tanh(2\theta_k) = \frac{2\sqrt{S^A S^B} \cos(ka)}{S^A + S^B}, \quad (15)$$

the Hamiltonian is finally diagonalized as

$$\begin{aligned}
H &= \sum_k \left[\epsilon_k^- \left(\alpha_k^\dagger \alpha_k + \frac{1}{2} \right) + \epsilon_k^+ \left(\beta_k^\dagger \beta_k + \frac{1}{2} \right) \right] \\
&- \frac{NJS^A}{2} (1 + \gamma), \quad (16)
\end{aligned}$$

where the two energy branches are

$$\epsilon_k^\pm = JS^A \left[\sqrt{(1 - \gamma)^2 + 4\gamma \sin^2(ka)} \pm (1 - \gamma) \right] \mp h_0, \quad (17)$$

with $\gamma = S^B/S^A < 1$. As mentioned before, contrast to the AFM case,¹⁴ the staggered field needs not be introduced in the present FIM case. Thus physical quantities can be calculated directly as long as the system parameters are known.

Similar to the case of a FIM spin chain under a *uniform* magnetic field,²⁵ the magnons with energy ϵ_k^- (ϵ_k^+) in the present case correspond to the ferromagnetic (antiferromagnetic) excitations. The energy gaps of these two branches are $\epsilon_0^- = h_0$ and $\epsilon_0^+ = 2JS^A(1 - \gamma) - h_0$, respectively. That is, a gap is induced by the applied field for the ferromagnetic excitations, while the gap of the antiferromagnetic excitations is reduced by the applied field. In the absence of external magnetic field, the ferromagnetic branch ϵ_k^- becomes gapless with quadratic k -dispersion at small k , which corresponds to the Goldstone mode due to the spontaneously broken rotational symmetry. Calculations using quantum Monte Carlo method yields nearly the same curve for ϵ_k^- , but ϵ_k^+ is separated from ϵ_k^- with a larger (k -independent) gap.^{19,22} Such a discrepancy is reduced when the spins are larger and the semiclassical formalism works better.^{22,26}

Since the magnons are non-interacting, it is straightforward to obtain the free energy ($k_B \equiv 1$)

$$F(\Omega) = T \sum_k \ln \left[4 \sinh \left(\frac{\epsilon_k^+}{2T} \right) \sinh \left(\frac{\epsilon_k^-}{2T} \right) \right] - \frac{NJS^A}{2} (1 + \gamma). \quad (18)$$

Furthermore, it can be explicitly shown that the longitudinal (gauge-invariant) spin current

$$I_s \equiv \left\langle \hat{m}_j \cdot \vec{I}_{j \rightarrow j+1} \right\rangle = - \frac{\partial F(\Omega)}{\partial \Omega}, \quad (19)$$

similar to the relation for persistent charge current in a normal metal ring, but with Ω replacing magnetic flux ϕ .^{13,14} From this relation we obtain the magnetization current,

$$I_m = \frac{g\mu_B}{\hbar} I_s = - \frac{g\mu_B}{L} \sum_{k, \alpha=\pm} v_k^\alpha \left(n_k^\alpha + \frac{1}{2} \right), \quad (20)$$

where

$$v_k^\alpha = \frac{1}{\hbar} \frac{\partial \epsilon_k^\alpha}{\partial k} = \frac{2JS^A a}{\hbar} \cdot \frac{\gamma \sin(2ka)}{\sqrt{(1 - \gamma)^2 + 4\gamma \sin^2(ka)}} \quad (21)$$

are the velocities of the magnons, and $n_k^\alpha = 1 / [\exp(\epsilon_k^\alpha/T) - 1]$ are the Bose occupation numbers.

III. BEHAVIOR OF THE PERSISTENT MAGNETIZATION CURRENT

For the FIM case, the magnetization current at $T = 0$ is nonzero even for vanishing magnon numbers (see

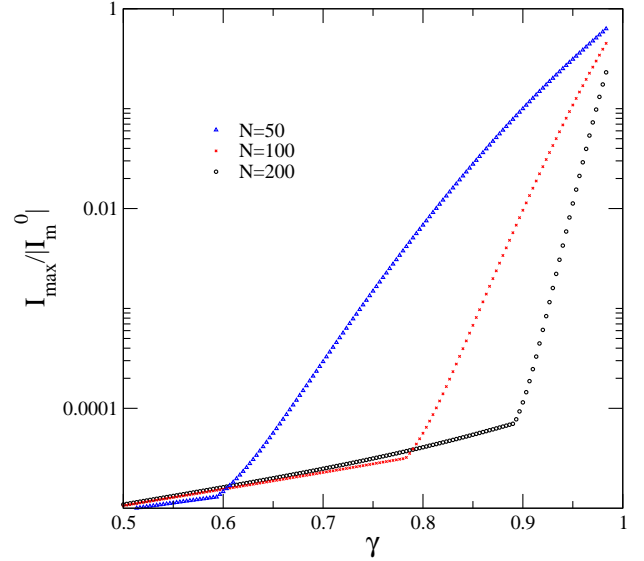


FIG. 2: Amplitude of the magnetization current at zero temperature as a function of γ , plotted for three different ring sizes.

Eq. 20), similar to the AFM case,

$$I_m = I_m^0 \sum_k \frac{\gamma \sin(2ka)}{\sqrt{(1 - \gamma)^2 + 4\gamma \sin^2(ka)}}, \quad (22)$$

where $I_m^0 \equiv -(2g\mu_B/\hbar)(JS^A/N)$. The magnon velocity within the summation is a periodic function of k . Therefore, after summing over the first Brillouin zone, the current is zero if the k -points are distributed symmetrically ($\Omega = \pi$). For other values of Ω , the summation is nonzero but the magnitude of the magnetization current decreases rapidly as $1 - \gamma$ becomes larger. Comparing with the AFM case,¹⁴ it can be seen that $\Delta \equiv \sqrt{(1 - \gamma)^2 + 4\gamma}$ plays a role similar to the Haldane gap, and its inverse determines the scale of the spin correlation length ξ . Therefore, when γ is small enough such that $\Delta \gg 2\pi/N$, the spin correlation length $\xi \ll L$; while if $\gamma \simeq 1$, such that $\Delta \ll 2\pi/N$, we have $\xi \gg L$. Therefore, by varying the ratio of the two different spins, qualitatively different regimes, $\xi \gg L$ and $\xi \ll L$, can be reached. In Fig. 2, the maximum amplitude of the magnetization current I_{\max} is plotted as a function of γ . The functional form of $I_{\max}(\gamma)$ shows a very clear crossover between these two different regimes.

Thermal energy could excite magnons and generate larger magnetization current. Typical influence of the temperature on the magnitude of the magnetization current can be seen in the inset of Fig. 3. We have also studied the dependence of I_{\max} on the parameters T , h_0 , and γ . From the magnon dispersion relations in Eq. (17), we expect activation behavior for $I_{\max}(T)$ at low temperature $T < \epsilon_0^- = h_0$. When the thermal energy is larger than the field-induced energy gap h_0 , $I_{\max}(T)$ should be proportional to T , similar to the behavior of the persistent spin current in a FM spin ring.¹³ These behaviors

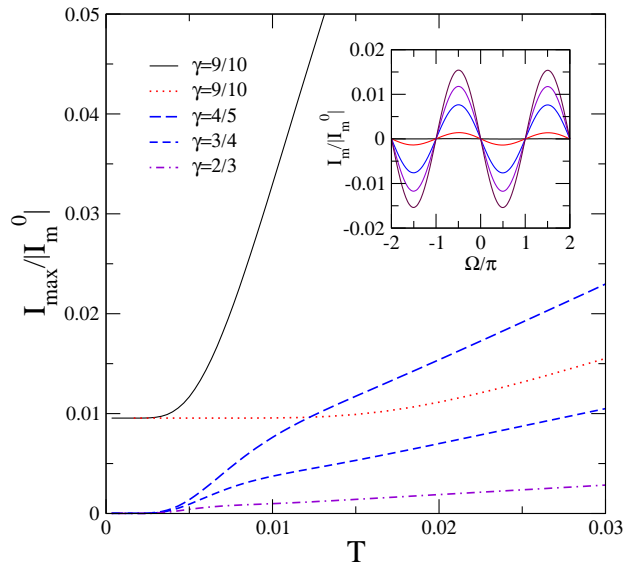


FIG. 3: Amplitude of the magnetization current as a function of temperature T . Solid (dotted) line corresponds to a system ($N = 100, \gamma = 0.9$) in a magnetic field $h_0/2JS^A = 0.01$ (0.05). Other curves with different γ all have $h_0/2JS^A = 0.01$. Inset: The variation of the magnetization current with respect to the change of Ω and T ($N = 100, \gamma = 0.8$). The temperatures for the curves with the smallest amplitude (indiscernible from the horizontal axis) to the largest amplitude are $T/JS^A = 0, 0.005, 0.010, 0.015, 0.020, \text{ and } 0.025$.

can be seen in Fig. 3. For the upper two curves with $\gamma = 0.9$, there is a significant amount of spin current at zero temperature and the activation behavior is implicit. Also, the persistent magnetization current at very low T is independent of the value of h_0 (see Eq. 22).

IV. CONCLUSION

We extend the work of Schütz *et al.*^{13,14} and studied the persistent spin current in a FIM spin ring. At $T = 0$, the functional form of the magnetization current $I_m(\gamma)$ shows distinctive behaviors above/below a threshold value of γ , which depends on the size of the ring. When thermal excitation can overcome the field-induced energy gap $\epsilon_0^- = h_0$, the magnitude of the spin current grows linearly with temperature T .

Both the persistent charge current in a metal ring and the persistent spin current in a spin ring are related to geometric phases (albeit of different origins). As in the case of the FM spin ring, the induced electric voltage would be of the order of nV , which poses a stringent experimental challenge. Recently, several types of FIM spin-chain compounds have been synthesized.^{27,28} To obtain a FIM spin chain with $\gamma > 0.8$, one might need to introduce rare earth elements,²⁹ or to fabricate a ring composed of magnetic molecules with large spins.³⁰

On the theoretical side, several questions remain open, such as the generalizations to quasi-1D spin rings or spin rings with itinerant electrons. The realistic effects of disorder, interaction, or contact leads remain unknown in the spin ring case. Further studies are desired.

Acknowledgments

J.N.W. and M.C.C. thank the support from the National Science Council of Taiwan under Contract Nos. NSC 93-2112-M-003-009 and NSC 94-2119-M-002-001. M.F.Y. acknowledges the support by the National Science Council of Taiwan under NSC 93-2112-M-029-006.

- ¹ M. Buttiker, Y. Imry, and R. Landauer, Phys. Lett. A **96**, 365 (1983); H. F. Cheung, Y. Gefen, E. K. Riedel, and W. H. Shih, Phys. Rev. B **37**, 6050 (1988); H. F. Cheung, Y. Gefen, and E. K. Riedel, IBM J. Res. Dev. **32**, 359 (1988).
- ² L. P. Levy, G. Dolan, J. Dunsmuir, and H. Bouchiat, Phys. Rev. Lett. **64**, 2074 (1990); V. Chandrasekhar, R. A. Webb, M. J. Brady, M. B. Ketchen, W. J. Gallagher, and A. Kleinsasser, Phys. Rev. Lett. **67**, 3578 (1991).
- ³ N. Byers and C. N. Yang, Phys. Rev. Lett. **7**, 46 (1961).
- ⁴ M. V. Berry, Proc. Roy. Soc. London A **392**, 45 (1984).
- ⁵ D. Loss, P. Goldbart and A. V. Balatsky, Phys. Rev. Lett. **65**, 1655 (1990); D. Loss and P. M. Goldbart, Phys. Rev. B **45**, 13 544 (1992).
- ⁶ Y. Meir, Y. Gefen and O. Entin-Wohlman, Phys. Rev. Lett. **63**, 798 (1989); O. Entin-Wohlman, Y. Gefen, Y. Meir and Y. Oreg, Phys. Rev. B **45**, 11 890 (1992).
- ⁷ H. Mathur and A. D. Stone, Phys. Rev. Lett. **68**, 2964 (1992); H. Mathur and A. D. Stone, Phys. Rev. B **44**, R10

I.

957 (1991).

- ⁸ Y. Aharonov and A. Casher, Phys. Rev. Lett. **53**, 319 (1984).
- ⁹ A. V. Balatsky and B. L. Altshuler, Phys. Rev. Lett. **70**, 1678 (1993).
- ¹⁰ M. Y. Choi, Phys. Rev. Lett. **71**, 2987 (1993).
- ¹¹ S. Oh and C. M. Ryu, Phys. Rev. B **51**, 13 441 (1995).
- ¹² D. Awschalom, N. Samarth, and D. Loss, *Semiconductor Spintronics and Quantum Computation* (Springer, Berlin, 2002).
- ¹³ F. Schütz, M. Kollar, and P. Kopietz, Phys. Rev. Lett. **91**, 017205 (2003).
- ¹⁴ F. Schütz, M. Kollar, and P. Kopietz, Phys. Rev. B **69**, 035313 (2004).
- ¹⁵ P. Bruno, Phys. Rev. Lett. **93**, 247202 (2004); V.K. Dugaev, P. Bruno, B. Canals, and C. Lacroix, Phys. Rev. B (in press); cond-mat/0503013.
- ¹⁶ D. Schmeltzer, A. Saxena, A. R. Bishop, and D. L. Smith, cond-mat/0405659.
- ¹⁷ W. Zhuo, X. Wang, and Y. Wang, cond-mat/0501693.
- ¹⁸ Y. Cheng, Y. Q. Li, and B. Chen, cond-mat/0505547.
- ¹⁹ S. Brehmer, H.-J. Mikeska, S. Yamamoto, J. Phys.: Condens. Matter **9**, 3921 (1997).

- ²⁰ S. K. Pati, S. Ramasesha, D. Sen, Phys. Rev. B **55**, 8894 (1997); J. Phys.: Condens. Matter **9**, 8707 (1997).
- ²¹ C. Wu, B. Chen, Xi Dai, Yue Yu, and Z-B Su, Phys. Rev. B **60**, 1057 (1999).
- ²² S. Yamamoto, cond-mat/0310004, also in *Recent Research Developments in Physics*, Vol. 4 (Transworld Research Network, Kerala, 2003), and references therein.
- ²³ If there are next-nearest-neighbor couplings in the Heisenberg model, then the local rotation performed on a particular site would depend on which neighbor it couples with.
- ²⁴ A. Shapere and F. Wilczek, *Geometric Phases in Physics* (World Scientific, Singapore, 1989). In the discrete case, the closed trajectory is connected by geodesics on the surface of the unit sphere from \hat{m}_j to \hat{m}_{j+1} .
- ²⁵ K. Maisinger, U. Schollwöck, S. Brehmer, H.-J. Mikeska, and S. Yamamoto, Phys. Rev. B **58**, R5908 (1998).
- ²⁶ S. Yamamoto, T. Fukui, and T. Sakai, Eur. Phys. J. B **15**, 211 (2000).
- ²⁷ N. Fujiwara and M. Hagiwara, Solid State comm. **113**, 433 (2000).
- ²⁸ A. S. Ovchinnikov, I. G. Bostrem, V. E. Sinityn, N. V. Baranov, and K. Inoue, J. Phys.: Condens. Matter **13**, 5221 (2001); A. S. Ovchinnikov, I. G. Bostrem, V. E. Sinityn, A. S. Boyarchenkov, N. V. Baranov, and K. Inoue, J. Phys.: Condens. Matter **14**, 8067 (2002).
- ²⁹ For example, Mn^{2+} with $S = 5/2$ and Cr^{2+} (or Mn^{3+}) with $S = 2$ can give $\gamma = 0.8$; Ho^{3+} with $J = 8$ and Dy^{3+} (or Er^{3+}) with $J = 15/2$ can give $\gamma = 0.937$. For other possibilities, see Sec. 3 of Yamamoto's review paper in Ref. 22.
- ³⁰ D. Loss, D. P. DiVincenzo, and G. Grinstein, Phys. Rev. Lett. **69**, 3232 (1992); J. von Delft and C. L. Henley, Phys. Rev. Lett. **69**, 3236 (1992); A. Garg, Europhys. Lett. **22**, 205 (1993).